



## PRINCIPLES OF CREATING A DIAMOND ABRASIVE TOOL TAKING INTO ACCOUNT THE FEATURES OF THE MICROCUTTING PROCESS

O.F. Salenko<sup>1\*</sup>, L.F. Golovko<sup>1</sup>, A.O. Salenko<sup>1</sup>, V.T. Shchetynin<sup>2</sup>, R.H. Arhat<sup>2</sup>, M.R.F. Budar<sup>3</sup>

<sup>1</sup>National Technical University of Ukraine "Igor Sikorsky Kyiv Polytechnic Institute", Kyiv, Ukraine

<sup>2</sup>Kremenchuk Michailo Ostrogradsky National University, Kremenchuk, Ukraine

<sup>3</sup>Central Ukrainian National Technical University, Ukraine

### ARTICLE INFO

#### Article history:

Received 5 November 2020

Accepted 3 December 2020

#### Keywords:

carbon-carbon materials; diamond tool, functional approach; processing, efficiency, surface clusters

### ABSTRACT

*The article discusses the creation of a modern diamond-abrasive tool for processing specific materials - carbon-carbon composites, which have high strength, temperature resistance, and low machinability. The anisotropy of the material structure, porosity, the tendency to crack formation with the release of a significant amount of dust makes the processing of such materials with traditional tools problematic. The application of a functional approach to the design of the working surfaces of the tool, including the non-rigid one (in the form of diamond threads, saws of the renovator), is proposed, which allows the cutting surfaces to be considered as a set of separate clusters, the functional properties of which are focused on ensuring maximum productivity in each specific zone of material processing. This significantly reduces dust contamination on the surface, improves and stabilizes the cutting process.*

© 2020 Journal of the Technical University of Gabrovo. All rights reserved.

### INTRODUCTION

The modern development of science-intensive production requires the increasing use of new composite materials – structural, heat-resistant, special purpose, etc., the processing of which, including diamond tools, faces a number of difficulties.

For the most widely used fiberglass and carbon plastics, carbon-carbon materials, these difficulties are caused by the presence in the composite structure of high-strength reinforcing fibers (carbon or highly modular glass), which impair the ability of the tool to control the processing area. As a rule, cutting of materials is long enough, and the used diamond tool changes its condition and its own cutting properties due to degradation. Such degradation is not uniform and proportional, and occurs mainly in areas where the processing conditions are quite different from the conditions of steady cutting. This feature is most fully manifested in tools such as diamond strings, nozzles for renovator, tubular drills. Therefore, it is easy to conclude that the increase in the efficiency of diamond tools is seen in the formation of a layer that would best meet the operating conditions of the cutting edges, which, based on the principle of decomposition, can be divided into conditional clusters of the surface.

In this case, based on the principles and foundations of the function-oriented approach, the development of conditions for effective processing of products from composite reinforced materials and binding the properties of the tool edges to a particular type of composite is an

effective method. Its implementation makes it possible not only to improve and stabilize the cutting conditions, but also to achieve a fuller use of the array of diamond grains, to increase the efficiency of the process as a whole. At the same time, ensuring long-term stability of microcutting on the basis of controlled molding by density, fractionality and method of putting a diamond-containing layer of the cutting surface of the tool will significantly increase the efficiency of processing.

### RESEARCH METHODS

Composites are used in the manufacture of aircraft, ships, in the automobile industry. Cheaper materials are used in the packaging industry, in the manufacture of household goods. Composites are actively used in tool production, and not only for creation of cutting plates (elements), but also for production of bases of, first of all, abrasive-containing (diamond-containing) tools. [1].

Heterogeneity of structure, difference of physical and mechanical properties of components not only provide wide opportunities in the field of formation of initial indicators and properties of a finished product [2], but also cause active search of new methods and ways of processing of materials [3,4], formation of properties of surface layers, which will determine the performance of the product during its operation.

The processing of composite materials is described in many papers of world leading scientists, in particular, such

\* Corresponding author. E-mail: salenko2006@ukr.net

as G. Mittal, K.Y. Rhee, A.S. Yuanyushkin, D.A. Rychkov, D.V. Lobanov, [5-9].

Thus, to increase the efficiency of processing composites, researchers focus on:

- creation of progressive designs of the cutting tool;
- application of modern tool materials, ceramics and superhard materials;
- the use of activators of the cutting/micro-cutting process by changing the state of the processing area;
- carrying out the actions for “designing” not only a product, but also the used material taking into account the further machining;
- development and implementation of hybrid processes capable of changing the conditions and types of controlled impact on the processed composite blanks.

While the first directions of improvement of processes of composites processing are known and quite widespread (they are based on the fundamental papers of the researchers of the Kharkiv and Kyiv schools of cutting, in particular, M.F. Semko, H.V. Shabalin, P.S. Redko, E.M. Levenberh, A.I. Hrabchenko, V.L. Dobroskok, V.A. Fedorovych, B.A. Perepelytsia et al. [10]-[13]), the next

three directions have lately begun to actively develop. In papers of V.M. Orel, O.O. Chencheva, Ye.Ye. Lashko (namely [14]) it is shown that a change in the load conditions of the cutting zone, a change in the stress state at the points of contact with the cutting or abrasive tool) can significantly reduce the resistance to destruction of the material.

However, greater possibilities for the rational use of diamond tools are provided by the use of function-oriented approach, described in detail in papers [15] – [17]. In this case all interactions in the technological system are considered as a manifestation of particular functions of the constituent elements, and the properties of the tool are formed locally and can change within the surfaces and their separate parts.

This enables considering the functional elements in a hierarchical scheme. In this case a tool set may consist of a functional set ( $TS$ )  $m_1 = \{f_{11}, f_{12}, f_{13}, \dots, f_{1v_1}\}$ , that may include any types of diamond tools (Fig.1). Here  $f_{1s1}$  – any functional element (product) of the 1st level of the hierarchical structure of the division,  $v_1$  – the power of the set of the  $m_1$  of the 1st level of division ( $v_1 = M$ ). If the process of division into functional elements is performed for one product, then  $v_1 = 1$ .

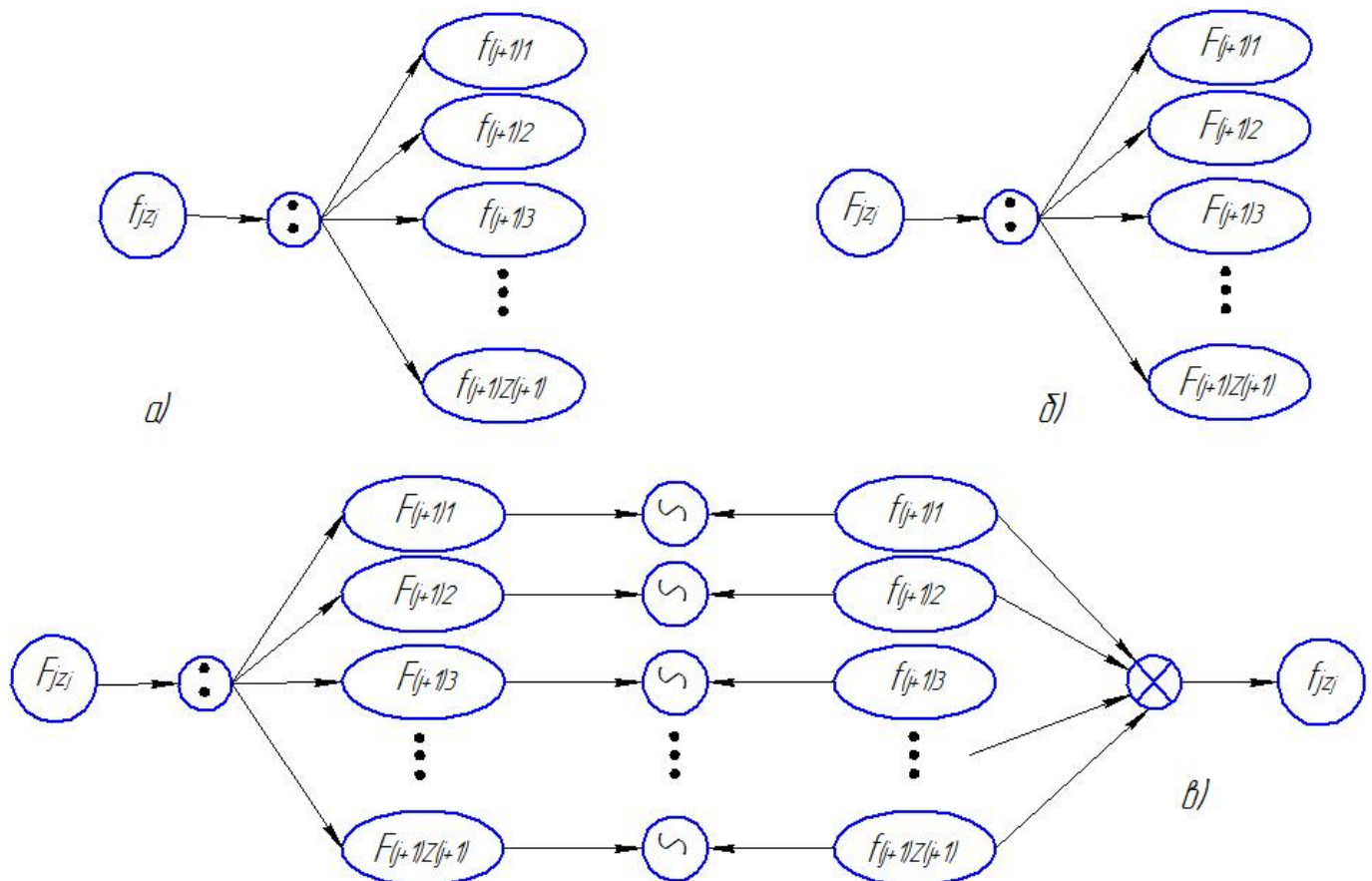


Fig. 1. Decomposition and synthesis of functional elements and functions:

a – the scheme of decomposition of the functional element of the  $j$ -th level of the depth of technology on the set of functional elements  $(j + 1)$ -th level; b – the scheme of decomposition of a complex function of the  $j$ -th level of technology depth into a set of functional elements  $(j + 1)$ -th level; c – the scheme of synthesis of functional elements of the product on the basis of a complex function.

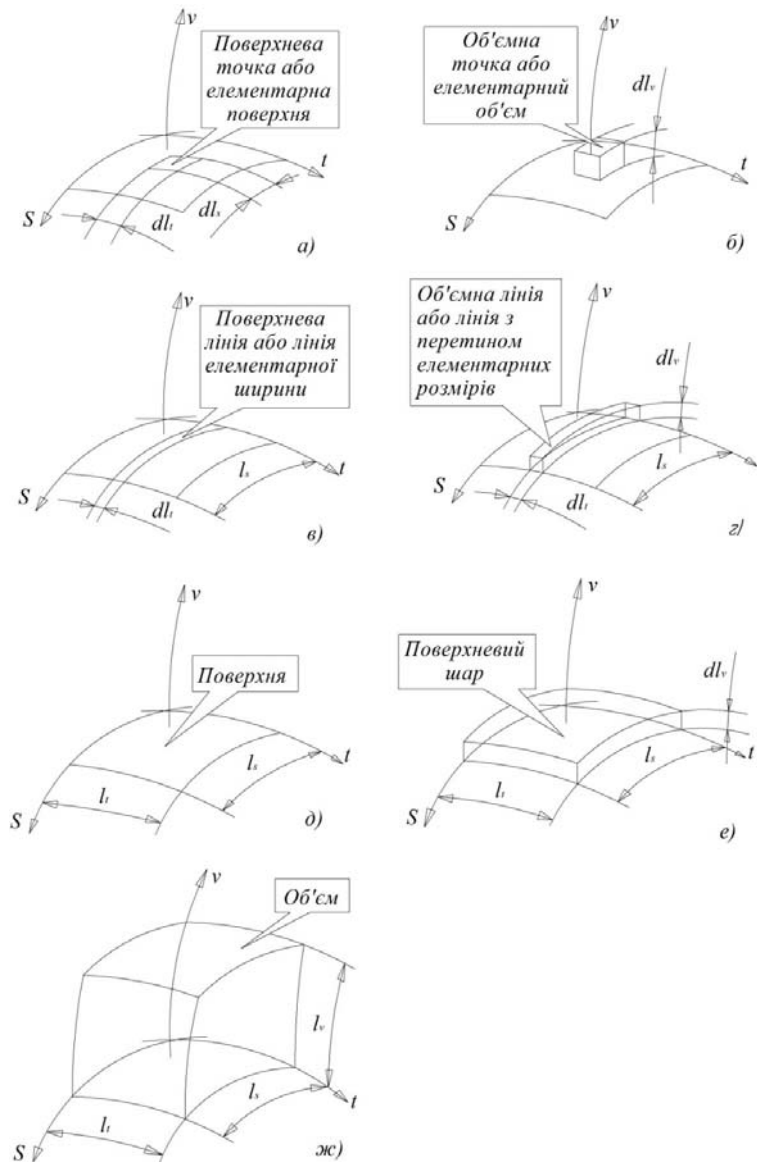


Fig. 2. Geometric interpretation of types of functional (executive) components of the *i*-th level of division of a cutting part of the tool: a) surface points or elementary surfaces; b) volumetric points or elementary volumes of the *i*-th level of division, the sizes of which are defined by operational parameters of the product; c) the surface lines or the lines of the elementary width; d) the volumetric lines or the lines with a cross section of the elementary sizes; e) the surfaces of the *i*-th level of division; f) the surface layers of the *i*-th level of division, the thickness of the layers of which is determined by the operational parameters of the product; g) volumes of the *i*-th level of division

As with such an idea for a set of products there is a set of functional parts  $m_i = \{f_{i1}, f_{i2}, f_{i3}, \dots, f_{ivi}\}$ , where  $f_{ivi}$  – any functional element of the *i*-th level of the hierarchical structure of the division,  $v_i$  – power of sets of the  $m_2$  *i*-th level of the division, each tool is divided into functional parts (functional elements of the *i*-th level of division), according to Fig.2.

Thus, it can be stated that the function-oriented approach is an effective highly efficient method for creating processing actions, especially those associated with the final formation of products from composite materials.

Usually the power loads of the diamond layer during the operation of the tool are significantly different and are determined by the scheme of interaction of the working surfaces with the workpiece. Thus, when milling the surface of the plates that form the cutting wedges, cutting force *R* is created. Its value and direction are determined by the relative motion of the wedge along the surface of the workpiece, as well as by the cross section of the removed chips. The latter directly depends on cutting depth *f*. The

contact conditions will change during the period of stability  $T_m$ , the changes will be caused by the phenomena of wear. Thus, the change of contact conditions will occur both as a consequence of periodic contact and as a consequence of processes and phenomena of wear.

For the front *P* and rear *Z* surfaces, representing the planes of the cutting wedge, the contact conditions will be described by the equations:

$$R_x, R_y, R_z = f(R_0), R_0 = \frac{c_p t^{x_p} s_z^{y_p} Bz}{D^{q_p}},$$

$$R_i = f(T, \alpha) = (R_0 + v_R T) \cos(\omega t), t = f(n), \sigma_p = \frac{R}{f_k},$$

$$\sigma_z = \frac{R_y}{f_k}, T < T_m, R_y = 0,55 R_0$$

That is, in addition to the periodic power load (at the time of entry of the plate into the workpiece and before its exit), the change in the geometry of the plate leads to a gradual increase in the maximum forces acting in the

system. There are no significant deformations in the technological system.

In contrast to milling, cutting materials with cutting wheels occurs with a constant change in the scheme of interaction. This is maximally traced when cutting tubular billets, in which the position of the contact points is constantly changing from the moment of insertion until the moment of the tool outside the billet. The cutting forces and, accordingly, the stresses in the surface layer will be

$$R_s = C_p v^{x_p} s^{y_p} t^{z_p}, \quad R_i = f(T, \alpha) = R_0 + v_R, \quad \sigma_p = \frac{R}{f_{kp}}$$

$$\sigma_b = \frac{R_y}{f_{kt}} \text{ and } f_{kp}, f_{kt} \text{ -contact areas determined by}$$

immersion of the circle in the body of the workpiece during the operating cycle. In this case, the heat released in the contact zone, in accordance with [18] may lead to deformation of the wheel and to an increase in cutting forces on the side surfaces.

A band or string tool is a tool with a non-rigid base; it works as a continuous flow of alternating cutting microclines. A variety of this tool are plates (blades), operating in oscillating mode and used in renovators.

In the general case we will consider that the used diamond tool for processing of workpieces from materials like KIMF possesses final rigidity. Then the hollow structure of the material will have a significant impact on the interaction conditions and on the processes and phenomena occurring in the cutting zone. When cutting 3D composite carbon-carbon materials the following is taken into account [19]:

- the structure of the material is hollow, with a hollowness of 3-7%;
- in three orthogonal directions the fibers are connected in bundles, the diameter of each is 1.25-1.8 mm;
- the combination of bundles and fibers into a single structure is performed by pyrocarbon obtained by hot precipitation.

Table 1 contains the basic properties of the material.

Let the non-rigid tool have a linear contact with the surface, and the scheme of interaction corresponds to Fig.3.

The equation of the elastic line on the initial section has the form

$$\varpi_z = -\frac{Pa^2b^2}{6EJl} \left( 2\frac{z}{a} + \frac{z}{b} - \frac{z^3}{a^2b} \right)$$

for concentrated load and for distributed (when immersed in the body)

$$\varpi_z = -\frac{qbl^3}{48EJ} \left[ 8\frac{d}{l} \left( \frac{z}{l} - \frac{z^3}{l^3} \right) - \frac{2ab^2}{l^3} - \frac{b^3}{l^3} + 2\frac{b^2}{l^2} \right],$$

where  $P$  and  $q$  – transverse concentrated and distributed load from cutting forces taking into account the pre-tension of the saw blade.

For a string, the resistance to bending of which is almost absent, the tension between the fasteners will be determined

by [20],  $= \frac{ql^2}{8f}$ ,  $f$  – maximum deflection when applying cutting force.

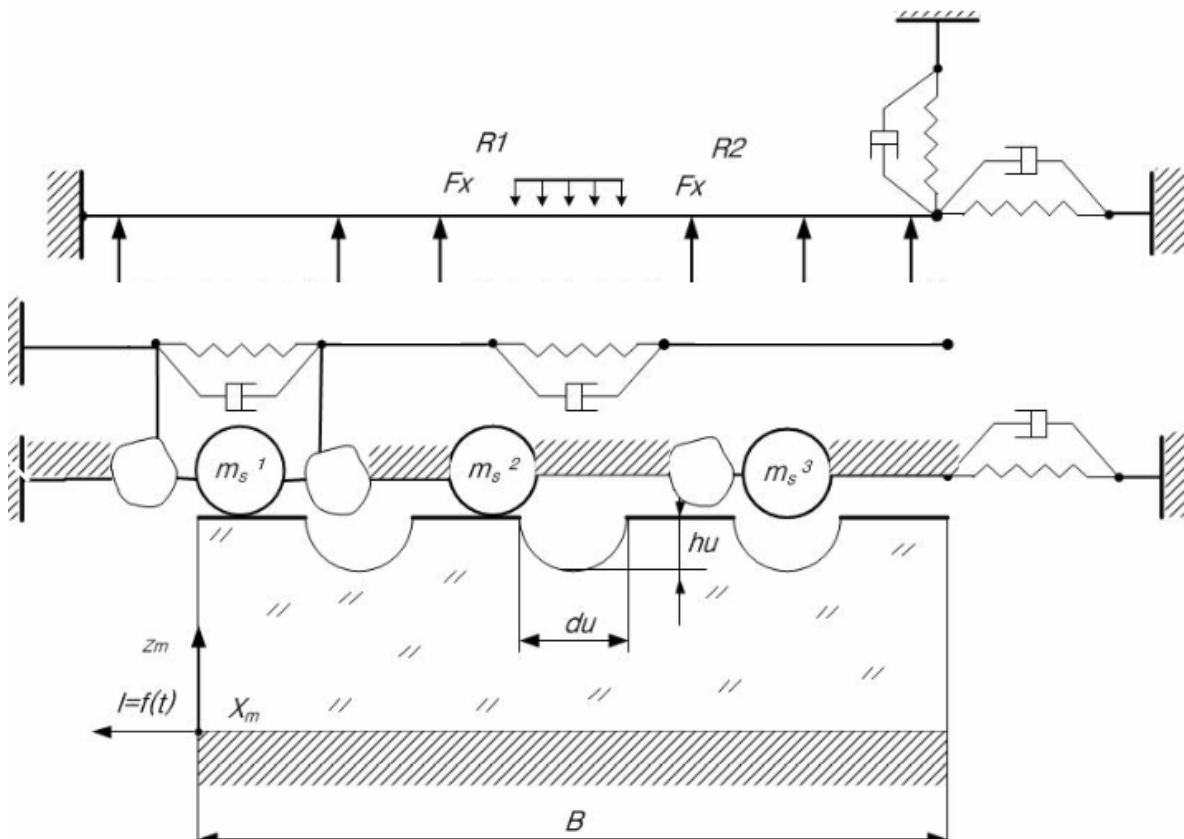
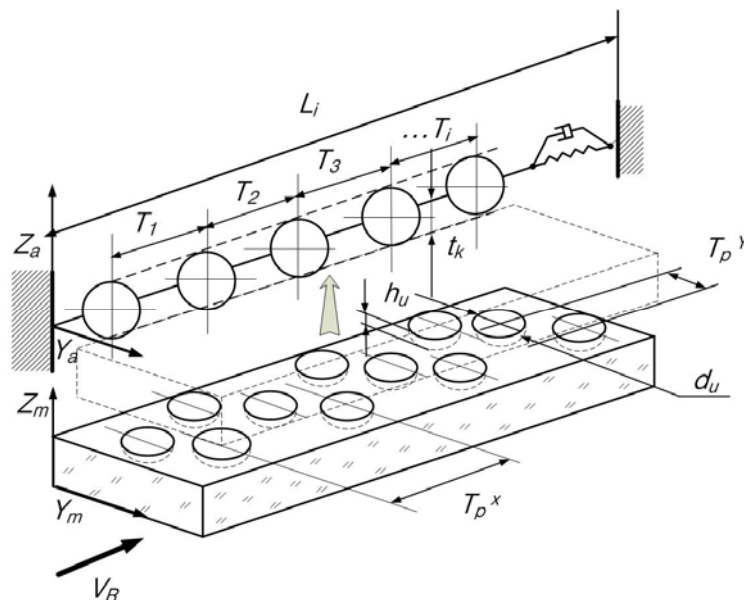


Fig. 3. The scheme of interaction of diamond grains and sludge particles with the workpiece surface

**Table 1** Basic mechanical properties of carbon fibers and the main technical characteristics of the fiber tow (according [20])

Characteristic	Carbon Fibers based on polyacrylonitrile			Carbon Fibers based liquid crystal pitch
	high strength	high elongation	highly modular	
Fiber diameter, nm	(7-9) $10^3$	(6-7) $10^3$	(6-9) $10^3$	$1 \cdot 10^5$
Tensile modulus, GPa	239-241	230-256	357-458	384-693
Tensile stress, GPa	3,0-3,5	4,0-4,5	2,0-2,5	2,1-2,4
Elongation at Tension,%	1,3-1,4	1,7-1,8	0,5-0,6	
Density, g / cm <sup>3</sup>	1,74-1,78	1,74-1,78	1,78-1,84	2,00
Specific strength, m	173-196	230-252	112-146	105-120
Linear Density (for CC CM)	350±50 (400±40) teks			
Breaking load, H, not less	45			
Bending strength in plastic, MPa, not less than	1078			
Modulus of elasticity in bending in plastic, MPa, not less	127,4			
Dynamic modulus of elasticity, GPa, not less	225			
Effective processing temperature of the tow °C, not less	1900			
Bulk density, g/cm <sup>3</sup> , not less	1,68			
Type of dressing	epoxy compatible			
Twist, no more	$15 \text{ m}^{-1}$			
Linear density	текс			

**Fig. 4.** The scheme for the simulation model of the interaction of the tool with a non-rigid surface layer (a) and the KIMF workpiece (b)**Table 2** Data for modeling

No.	Parameter	Measurement units	Value
1	Workpiece size $B \times L \times H$	mm	100×50×10
2	String length $L$	mm	250
3	Grain location step $T_1-T_i$	mm	1.5...2.5
4	Step between depressions $T_p$	mm	1.8
5	Depression diameter $d_u$	mm	1.2
6	Depth $h_u$	mm	0.2
7	Fraction of diamond grains	μm	150/200
8	Extension over the bundle	μm	50
9	The force of pressing the string on the outer points $P$	N	80
10	Velocity of motion $v_x$	m/s	1.2

The forced transverse oscillations of the particle carrier, which can be represented as a movable non-rigid rod with a constant cross section, are satisfactorily described in Euler variables by differential equations in partial derivatives

$$\frac{\partial^2 u}{\partial t^2} + 2v \frac{\partial^2 u}{\partial x \partial t} + v^2 \frac{\partial^2 u}{\partial x^2} - \frac{N(t)}{m} \frac{\partial^2 u}{\partial x^2} + \beta^2 \frac{\partial^4 u}{\partial x^4} = \varepsilon f(x, t) \quad (1)$$

where  $u(x, t)$  – transverse movements of the carrier with the coordinate  $x$  at the current moment of time;  $\varepsilon$  – the parameter of small disturbing force in comparison with force of action  $\beta^2 = \frac{EI}{m}$ ;  $m$  – mass per unit length of the saw blade;  $E$  – modulus of elasticity of the material;  $I = \frac{Bs^2}{12}$  – the moment of inertia of the cross section of the blade relative to the central axis;  $B$ ,  $s$  – the width and height of the cross section of the saw blade;  $N(t)$  – variable tensile strength of the non-rigid rod depending on the cutting conditions.

The solution of the given differential equation is carried out for boundary conditions having the form:

$$u = 0, x = 0, x = l; \frac{\partial^2 u}{\partial x^2} = 0, x = 0, \frac{\partial^2 u}{\partial x^2} = 0, x = l, \quad l - \text{the}$$

length of the analyzed section.

Perturbations will be determined by alternating the moments of grains contact with the processed fiber bundle and the gap  $f(x, t) = H \sin(\omega t)$ , where  $H$ ,  $\omega$  – the amplitude and frequency of perturbations.

Taking into account the fact that the variable force of tension of the rod will be determined by the forces of cutting resistance  $N(t) = N_0 + \varepsilon N_1 \cos(\mu t)$ , where  $N_1$  and  $\mu$  – parameters that are determined by the operating conditions and depend on the frequency of interaction of an individual grain with the surface, as well as the number of grains that are simultaneously in the contact zone, the system of differential equations that describe the basic parameters of oscillation will look like:

$$\begin{aligned} \frac{d\alpha}{dt} &= -\frac{\varepsilon}{(\omega + 0,5\mu)} \left[ \frac{\alpha H_2 \omega^2}{2} \sin 2\gamma + H_3 \cos \gamma \right] \\ \frac{d\gamma}{dt} &= \omega - 0,5\mu - \frac{\varepsilon}{(\omega + 0,5\mu)} \left[ \frac{H_2 \omega^2}{2} \cos 2\gamma + \frac{H_3}{\alpha} \sin \gamma \right] \end{aligned} \quad (2)$$

The solution of the given system makes it possible to determine the laws of motion of rod elements in angular coordinates and to determine conditions of occurrence of resonant phenomena. In addition, taking into account the geometric parameters of the contact zone enables determining the changes in the working loads of the tops of the cutting wedges (e.g. saw blade) and diamond grains.

Fig. 4a contains a simulation model of the tool interaction with the processed surface, 4b – a workpiece made of KIMF material, Table 2 contains data for modeling.

Therefore, the difference between the conditions of interaction of particles in the sections I...III is significant, which makes it possible to predict the effectiveness of the modification of the tool surface on a functional basis. In this case the following is considered. Let surface  $P$  of the workpiece consist of a number of functional zones  $Z_{ij}$ , that

differ in their properties  $V_{ij}^f$  and enable operation of functions  $FR_k$ .

The properties of each of the zones are determined by the operating conditions: power  $R_{ij}^{xy}$  and thermal  $T_{ij}^{xy}$  loads, the course of the phenomena of chemical interaction  $H_{ij}^a$ , the mechanisms of damage  $D_{ij}$ . Since all functional areas belong to one surface (and in the general case – to the volume of the object under consideration), i.e.  $Z_{ij} \in P$ , and the surface is set by function  $z = g(x, y)$ , that has a definition area  $R$ , and  $P = \iint_R dR$ , we have:

$$P = \iint_R \sqrt{1 + \left(\frac{\partial z}{\partial x}\right)^2 + \left(\frac{\partial z}{\partial y}\right)^2} dx dy \quad (3)$$

or for the case of an axisymmetric body (carrier of diamond grains – an elastic rod)  $P = \iint_R dP = \int_{\alpha}^{\beta} \int_{h(\Theta)}^{g(\Theta)} r dr d\Theta$ .

Then the change in surface properties can be determined on the basis of functional conditionality

$$V_{ij}^f = f\left(R_{ij}^{xy}, T_{ij}^{xy}, H_{ij}^a, D_{ij}\right)$$

for any second-order surface having the form  $F(x, y, z) = 0$  and at the intersection of the plane gives the equation of the curve of the second order of the form

$$\frac{x^2}{\left(a\sqrt{1 - \frac{h^2}{c^2}}\right)^2} + \frac{y^2}{\left(b\sqrt{1 - \frac{h^2}{c^2}}\right)^2} = 1$$

in projection on the selected axis within  $(x_1, y_1)$ ,  $(x_2, y_2)$  can be transformed to the form

$$\begin{aligned} V_R^f &= b_0^R + b_1^R x^2 + b_2^R xy + b_3^R y^2 + b_4^R x + b_5^R y \\ V_T^f &= b_0^T + b_1^T x^2 + b_2^T xy + b_3^T y^2 + b_4^T x + b_5^T y \\ V_H^f &= b_0^H + b_1^H x^2 + b_2^H xy + b_3^H y^2 + b_4^H x + b_5^H y \\ V_D^f &= b_0^D + b_1^D x^2 + b_2^D xy + b_3^D y^2 + b_4^D x + b_5^D y \end{aligned} \quad (4)$$

Thus, we obtain a family of continuous curves, which belong to the planes intersecting the body at certain angles and which reflect the change of properties in a certain direction from the selected starting point. Theoretically, such changes can occur infinitely, and are described by a curve of the second or even third order. However, in engineering practice, such differences as seen in the escape of particles by the value of  $h$ , located on a certain section of the plane in the number of  $w$ , will be determined by the size of the conditional cluster, i.e., the area where the application of particles remains predictable and controlled. Such areas can be repeated with different steps  $t$ , and the method of application – laser thermodeformation sintering – ensures the accuracy and reproducibility of such clusters on the working planes of the tool.

The formation of the cutting surface cluster is determined by the processes of heating and melting of the base material, the filler metal by laser radiation, coordinated gas transport of particles into the melt bath, mechanical pressure and movement of the irradiation point along the line defined by equation (4). All these processes are dynamic and have different degrees of activity.

Consider the process of heating the surface of the body with a solid-state laser that falls on the surface for some time and creates a local heating of the irradiation zone. In this case the energy density that will be absorbed can be determined by expression [21]:

$$q(x) = q_0 \exp\left(-x^2/r^2\right), \quad (5)$$

where  $q_0$  – the density of the power of the radiation in the center of the focus spot;  $r$  – the radius of the beam taking into account the distribution of radiation density in accordance with Gauss's law.

The heat distribution on the absorption surface of radius  $r$ , for example during perforation, is determined by the following equation:

$$T(x, z, t) = \frac{q_{max} r^2}{K} \left(\frac{a}{\pi}\right)^{1/2} \int_0^t \frac{P(t-t') dt' \exp\left[\frac{z^2}{4at} - \frac{x^2}{4at'}\right]}{\sqrt{t'(4at' + r^2)}},$$

where  $q_{max}$  – maximum radiation power density in the center of the spot;  $x$  – radial distance from the center of the heat source;

$$P(t) = q(t)/q_{max},$$

the temperature on the surface of a semi-infinite body at a point with coordinates  $(x, y, z)$ , provided that the laser beam moves along the surface at speed  $v$ , and provided that the heat loss from the surface is neglected, is defined as

$$\bar{T} = \frac{16}{\sqrt{\pi}} \int_0^{\infty} \frac{1}{\sqrt{(c'^2 + t'^2)(b'^2 + \bar{t}'^2)}} \exp\left[-\frac{(2\bar{x}'^2 + \bar{v}'t')^2}{4(c'^2 + \bar{t}'^2)} - \frac{\bar{y}'^2}{\bar{b}'^2 + \bar{t}'^2} - \frac{\bar{z}'^2}{\bar{t}'^2}\right] dt', \quad (6)$$

where  $\bar{T} = 16\sqrt{\pi K r T} / PA_0$ ;  $\bar{v} = v_r / 2a$ ;

$$\bar{x}' = \frac{x}{r}; \quad \bar{y}' = \frac{y}{r}; \quad \bar{z}' = \frac{z}{r}; \quad \bar{c}' = \frac{c}{r}; \quad \bar{b}' = \frac{b}{r}; \quad r^2 = cb;$$

$A_0$  – reflectivity of the workpiece material;  $P$  – laser radiation power;  $b, c$  – parameters of the power density distribution of laser radiation (according to Gauss's law).

The process of thermal conductivity in the volume of the workpiece material, which is limited by area  $\Omega$ , with surface  $\partial\Omega$ , can be described using:

- scalar temperature field:

$$T = T(P, t),$$

- heat flow vector field:

$$q = q(P, t) \rightarrow P = \{(x, y, z)\} \in \Omega,$$

- and a scalar field with specific thermal energy:

$$e = e(T).$$

Boundary conditions on external surfaces at  $\tau > 0$

$$\left\{ \Gamma_1 : -\lambda \frac{\partial T}{\partial n} = q_r; \Gamma_2 : \frac{\partial T}{\partial n} = 0; \Gamma_3 : -\lambda \frac{\partial T}{\partial n} = \alpha(t - t_{medium}); \right.$$

Conditions on the boundary of contact  $\Gamma_4$  at  $\tau > 0$ :

$$\left\{ \begin{aligned} t|_{\partial_4^-} &= t|_{\partial_4^+}, \\ -\lambda_- \frac{\partial T}{\partial n}|_{\partial_4^-} &= \lambda_+ \frac{\partial T}{\partial n}|_{\partial_4^+} \end{aligned} \right.$$

$$\left\{ \begin{aligned} t < t_m - \frac{\Delta t}{2}, \lambda_I(t) &= \lambda_s; [c_p(t)\rho(t)]_I = c_{ps}\rho_s; \\ t_m - \frac{\Delta t}{2} \leq t \leq t_m + \frac{\Delta t}{2}, \lambda_I(t) &= \lambda_s + \frac{\lambda_m - \lambda_s}{\Delta t} \left(t - t_m + \frac{\Delta t}{2}\right); \\ [c_p(t)\rho(t)]_I &= c_{ps}\rho_s + \frac{c_{pm}\rho_m - c_{ps}\rho_s}{\Delta t} \left(t - t_m + \frac{\Delta t}{2}\right) + \frac{L_f}{\Delta t}; \\ t > t_m + \frac{\Delta t}{2}, \lambda_I(t) &= \lambda_m; [c_p(t)\rho(t)]_I = c_{pm}\rho_m; \end{aligned} \right. \quad (7)$$

where  $n$  – normal to the surface;  $q_r$  – power density;  $\alpha$  – heat transfer coefficient;  $\Gamma_1$  – irradiated surface,  $\Gamma_2$  – surface of axial symmetry,  $\Gamma_3$  – surfaces in contact with the external environment,  $\Gamma_4$  – the contact boundary of the connector and the matrix.

In the boundary mode of evaporation, the size of the formed cavity depends on the total energy supplied to the surface layer of the processed workpiece. Diamond particles are fed into the formed cavity by the action of gas flow.

The movement of particles in the supply channel is caused by the transmission of external forces impulse in area  $\Delta l$  from the gaseous medium and is described by equation:

$$[F \cdot (p - \Delta p) - F_p] \cdot \Delta t = \Delta p \cdot F \cdot \Delta t,$$

where  $F$  – the cross-sectional area of the pipe supply of abrasive particles and diamonds. The change in the amount of mass movement of the two-phase flow on section  $\Delta l$  is

$$[\varepsilon \cdot \rho_T + (1 - \varepsilon) \cdot \rho_B] \cdot [F \cdot v_{cm} \cdot u_{y\partial} \cdot \Delta t + F \cdot v_{cm}^2 \cdot \Delta t],$$

where  $\rho_T, \rho_B$  – the density of solid particles and compressed air, respectively;  $\varepsilon$  – the volume fraction of solid particles in the aeromixture;  $1 - \varepsilon$  – the volume fraction of air in the aeromixture;  $\varepsilon \cdot \rho_T + (1 - \varepsilon) \cdot \rho_B = \rho$  – two-phase flux density;  $u_{y\partial}$  – the speed of sound propagation in a two-phase flow.

Therefore, with a fixed operating element, the size of the cluster will be determined by the melt zone and will have an axisymmetric shape.

The formation of surface clusters when supplying the operating elements relative motion requires taking into account the dynamics of displacements, Fig. 6. The system of differential equations describing the behavior of the feed drive, represented as a two-mass system with a stepper motor, has the following form:

$$\text{equilibrium of the first concentrated mass } \frac{d\varphi_1}{dt} = \omega_1;$$

equilibrium of the second concentrated mass

$$\frac{d\omega_2}{dt} = \frac{(c_{12}(\varphi_1 - \varphi_2) + b_{12}(\omega_1 - \omega_2)) - M_t - c_{34}(x_z - x_p) - b_{34}(v_z - v_p)}{J_2}$$

$\frac{d\varphi_2}{dt} = \omega_2$ , the equilibrium of the longitudinally moving table will be determined by equation:

$$m_p \frac{dv_p}{dt} = c_{34}(x_z - x_p) + b_{34}(v_z - v_p) - F_t, v_z = \omega_2 \frac{t}{2\pi}$$

where  $m_p$  – the mass of the table;  $F_t$  – nonlinear friction force in the guides of the work table;  $x_p, y_p$  – the coordinate and speed of the table;  $x_z, v_z$  – the coordinate and speed, which is determined by the movement of the

lead screw ;  $M_f$  – the moment of friction in the supports of the master kinematic link, which in general form will be a nonlinearity  $M_f = \text{sign} \omega_2 |M_f|$

The mathematical model of the stepper electric drive in dynamic mode will look in the following way:

$$\begin{aligned} \frac{d[i_1]}{dt} &= [L_1]^{-1} \{ [u_1] - [R_s][i_1] - \omega [K_{\omega 2}] - [\Psi_{M1}] \}, \\ \frac{d[i_2]}{dt} &= [L_2]^{-1} \{ [u_2] - [R_s][i_2] - \omega [K_{\omega 1}] - [\Psi_{M2}] \}, \\ M_{\mathcal{D}} &= -\Psi_M \cdot i_1 \cdot \sin p \theta - \Psi_M \cdot i_2 \cdot (\sin p(\theta - \lambda)) \\ \frac{d\omega}{dt} &= \frac{p}{J_{\Sigma}} (M_{\mathcal{D}} - M_C) \\ \theta &= p \int_0^t \omega dt = p\lambda \end{aligned}$$

where:  $J_{\Sigma} = J_{\Sigma} + J_{\Sigma}$  – the total moment of inertia of the electric drive reduced to the rotor shaft;  $p$  – number of pole pairs;  $\omega = \frac{d\theta}{dt}$  – rotation frequency;

$M_c = M_H + M_m + M_n$  – the total torque of the motor;  $M_H$  – moment of load resistance,  $M_m = D \frac{d\theta}{dt}$  – the moment of resistance of viscous friction (where  $D$  – coefficient of viscous friction),  $M_n$  – the moment of sliding friction in the bearings;  $[i_1], [i_2]$  – the matrix of the unknown (stator currents);  $[u_1], [u_2]$  – voltage matrices;  $[R_s]$  – the matrix of active resistances;  $[L_1], [L_2]$  – the direct matrices of differential inductances as a function of phase currents and the current position of the rotor;  $[K_{\omega 1}], [K_{\omega 2}]$  – matrices of coefficients of anti-EMF as a function of phase currents and the current position of the rotor;  $\omega$  – rotor rotation frequency,  $[\Psi_{M1}], [\Psi_{M2}]$  – the maximum value of flux linkage created by a permanent magnet,  $M_{\mathcal{D}}$  – the electromagnetic moment generated by the stator phase windings;  $M_c$  – moment of resistance of the motor;  $J_{\Sigma}$  – total inertia moment of ED;  $\theta, \lambda$  – mechanical and electrical angles;  $p$  – number of pole pairs [22].

## COMPUTER SIMULATION PROCESSES

For the string used for cutting materials such as KIMF a number of heat distribution diagrams are constructed, an example of which is given in Fig. 5.

It was found that the speed of working movements will directly determine the expected size of the cluster, because, as shown in Fig.6, with increasing speed also increases the error of reproduction of movements, and, consequently, the accuracy of the position of the point source at any given time relative to the treated surface.

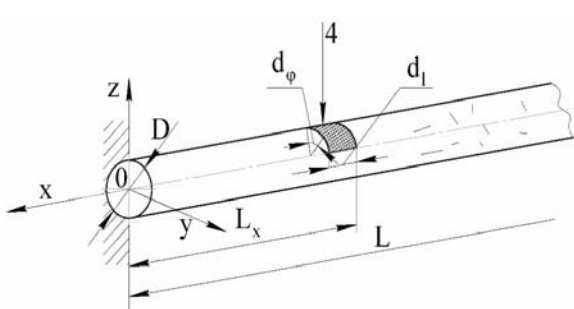


Fig. 5. The calculated model of string irradiation and diagram of heat distribution on the surface in a stationary system

As the size of the cluster is influenced by several active factors, a multifactor research was performed to obtain the appropriate regression equations of the expected values of the size of cluster  $F$ .

The factors taken into account are summarized in Table 3.

To obtain the model, a matrix of the plan of experiment  $2^5$  was generated in two blocks, which necessitated the implementation of 32 model experiments, according to Table 3.

From the performed analysis it follows that the most significant factor is temperature  $T$ , which actually determines the zone of melting of the filler material and heating of the surface of the base on which the diamond grains are fixed. The growth of this factor leads to an increase in the size of the cluster. The rate of thermal transfer  $\nu$  has the same tendency, which also leads to growth of  $F$ .

The effect of particle size is interesting. From Fig.7 it becomes obvious that there is a certain rational particle size at which the cluster can be minimized in size. In the accepted range of sizes it is most expedient to use particles of  $\rho = 75 \dots 10 \mu\text{m}$ . The gas pressure of the transport of the filler and particles in the treatment zone and the force of mechanical pressing  $p$  have no special effect.

Modeling the interaction of the string with the surface allowed establishing the condition of interaction of the non-rigid tool (string) with the porous surface layer of the workpiece (according to Fig. 4), Table 4.

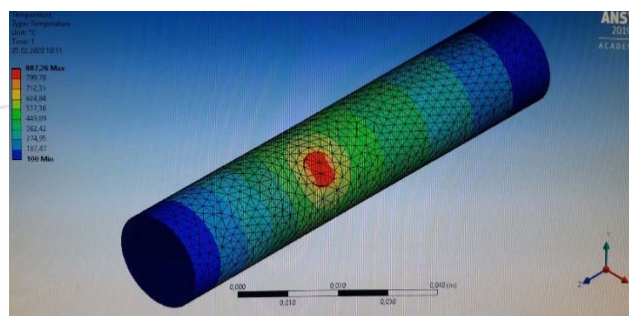
For the simulation the authors measured the intensity of the power load in different sections I... III, assuming that the speed is constant and equal to ... and the pressing force of diamond particles is determined by the vertical force  $P$  applied to two points **A** and **B**; the particles are fixed on the string, which is elastically deformable.

## EQUIPMENT FOR EXPERIMENTS

To ensure a steady process of laser thermodeformation sintering, a universal laser-jet complex LSK 400-5 [4] is used, on which an auxiliary device in the form of a module of longitudinal movement and a rotary table for installation of blanks is installed.

Universal laser-jet complex LSK-400-5 is equipped with a solid-state Nd: YaG laser with a power of 0.5 kW, with a wavelength of 1069 nm, with a pulse repetition frequency of 50-750 Hz.

The laser has a focusing system and a system for transporting the beam in the form of "flying optics", with means of interrupting the beam, as well as a number of auxiliary systems with which it is possible to implement jet laser, cryogenic and hydroabrasive processing.



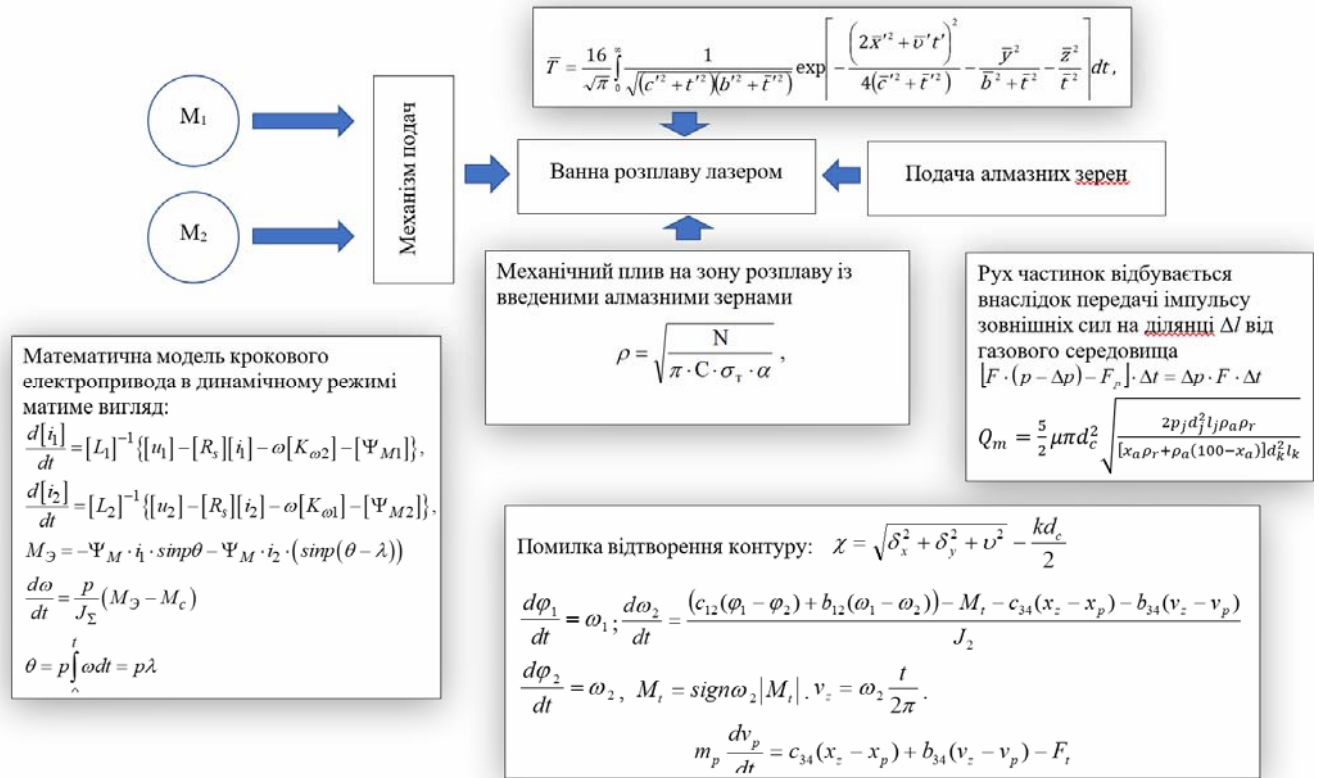


Fig. 6. Cluster formation with a mobile heat source

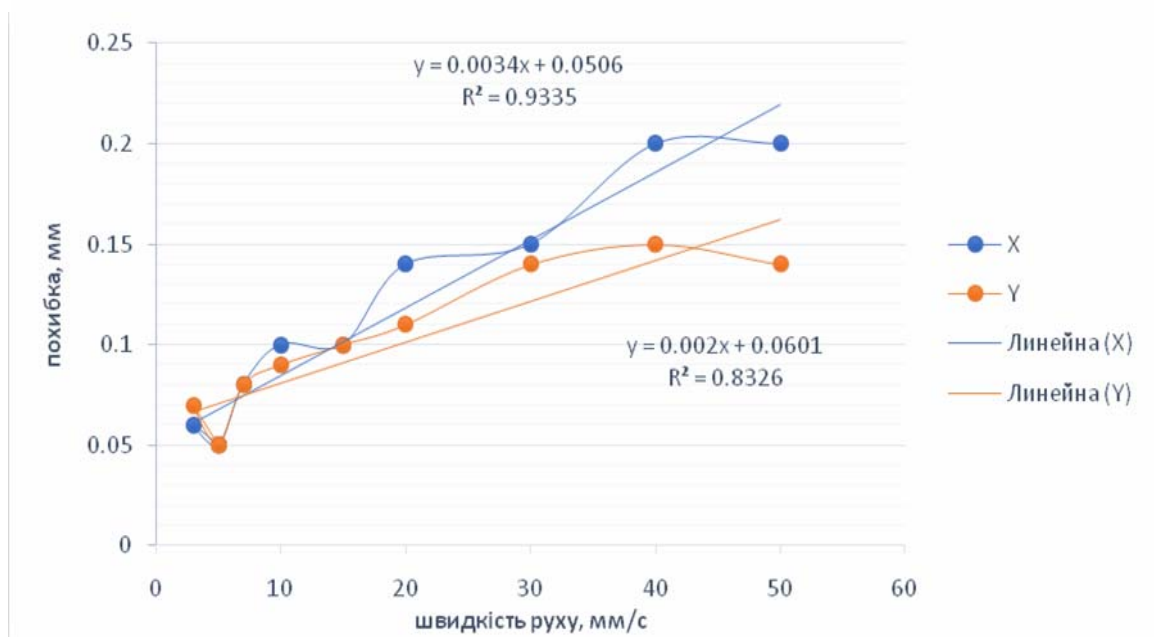
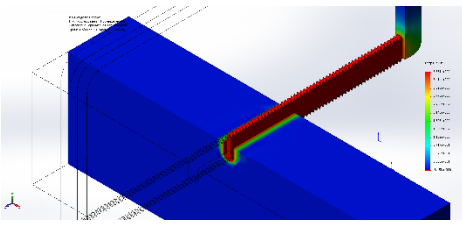
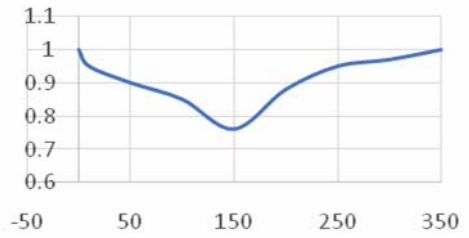
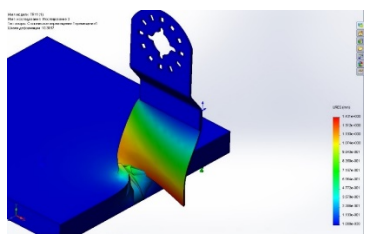
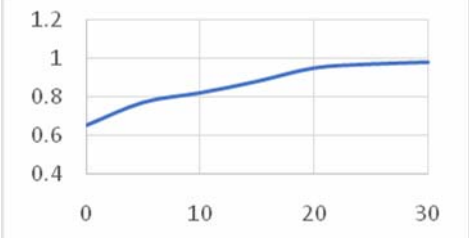
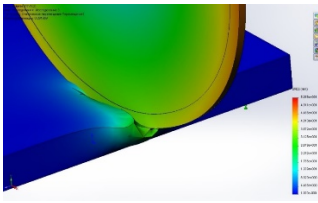
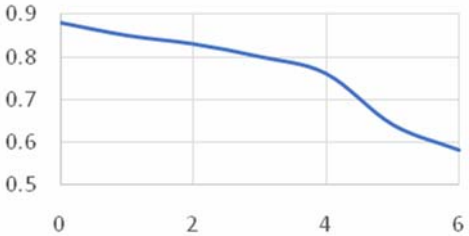


Fig. 6. Dependence of the error of reproduction of movements by the speed of movement of the operating element – a means of manipulating the workpiece

Table 3 Factors taken into account

	Parameter	Designation	Dimension	-	+	Note
1	Speed of movement	$v_i$	m/s	0.002	0.015	
2	Mechanical impact	$N$	N	50	150	
3	Gas pressure	$p$	MPa	0.01	0.08	
4	Particle size	$\rho$	$\mu\text{m}$	50	150	
5	Surface temperature	$T$	K	1100	1350	

**Table 4** The results of modeling the interaction conditions and the expected level of wear of the working edges of the tool

No.	Simulation conditions	Calculation results	Wear of working surface
1	2	3	4
	$V_p=0.4$ m/s; $P_h=80$ N; $n=60$ ; $d_r=3.5$ mm;		
	$V_p=12$ m/s; $P_h=80$ N; $n=3200$ r <sup>-1</sup> ; $l_r=5.0$ mm;		
	$V_p=50$ m/s; $P_h=25$ N; $n=4800$ r <sup>-1</sup> ; $d_r=125$ mm;		

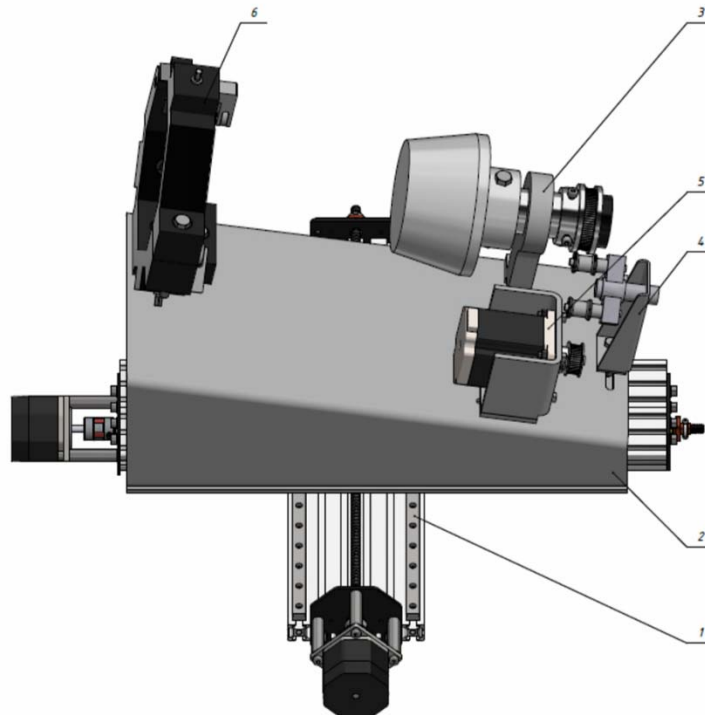


Fig. 8. Equipment ensuring the complex movement of the workpiece in the formation of surface clusters  
 1 – automated cross table that provides movement in the longitudinal and transverse directions; 2 – the plate is made of sheet material on which the unit of rotation of the workpiece is mounted – 3, rotation drive – 5, toothed belt tensioning mechanism – 4. A lunette is installed to fix the workpiece in the axial direction – 6.

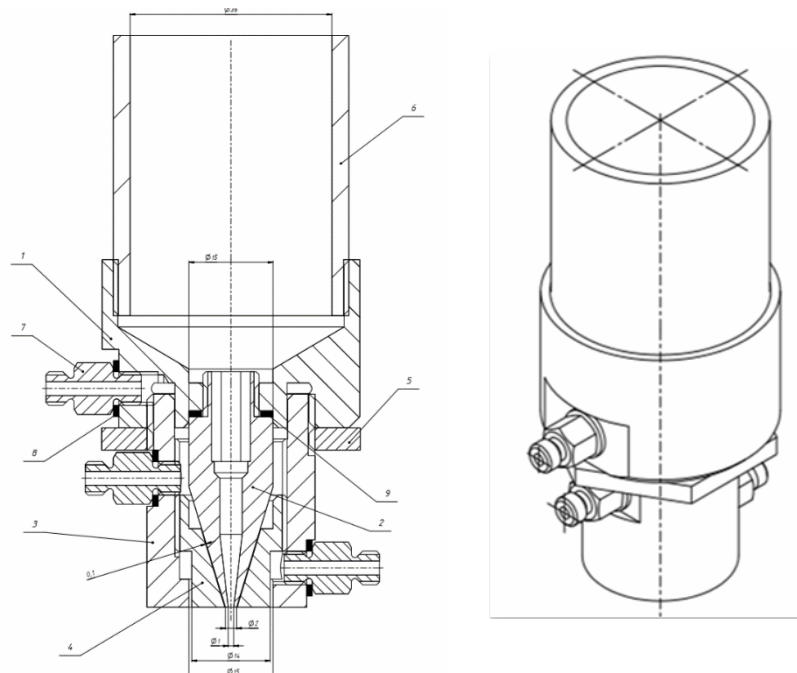


Fig. 9. Heads for feeding the abrasive and additive material in the treatment area

A special device (Fig.8) has been developed to perform operations of controlled diamond laying, which provides simultaneous rotational and longitudinal gradual movement of the tool along a given trajectory. The system of laptop with drivers for stepper EMX-142 motors works.

A gas-throttle conveying device was used to introduce diamond particles into the working area. The working head was made in two versions: with lateral supply of filler material and diamonds and coaxial, i.e. the supply of diamond particles is carried out by gas flow through an adjustable annular nozzle, in which the focused laser beam travels along the central axis.

Additionally, a filler powder material (based on fine Ni powder) is fed into the surfacing zone. The used device makes it possible to transport a mix of components – diamond grains and powder of filler metal.

The research of the condition of the surface of the instrument after its manufacture, as well as after processing was carried out using scanning electron microscopy using the device PEM-106-II.

## THE OBTAINED RESULTS AND DISCUSSION QUESTIONS

Comparison of model and experimental results on surface properties showed relatively high convergence of results (error is 12-15%). Thus, it was found that the formation of surface layer clusters on experimental equipment with a step between grains of 100  $\mu\text{m}$  and 150  $\mu\text{m}$  and the distance between clusters greater than 2.0 mm is quite stable, without significant grain damage, without significant yield of filler metal. Scattering of laying parameters is  $\pm 35 \mu\text{m}$ , larger dispersion of the parameter is inherent in the higher fractionality of the used diamond powder (30-50  $\mu\text{m}$  and 50-75  $\mu\text{m}$ ), Fig. 10.

Microelectronic study of the tool surface formed using an annular nozzle and filler solder with particle fractions of 10/20  $\mu\text{m}$ , as well as diamond grains with a fraction of 75/100  $\mu\text{m}$  showed that adjusting the flow of filler materials traveling through two channels, enables obtaining sufficiently homogeneous surface diamond-containing

layers. The binder was completely molten, and covered the surface of the base of the tool with a layer 25-40  $\mu\text{m}$  thick. The raster shows the inclusion of dirt, which apparently got into the treatment area due to contamination of the working gas supply channel.

The application of reversible surface engineering and the determination of functional differences in microcutting conditions based on the results of modeling and studying the wear intensity of the cutting edge of a traditional tool – strings type APP-22m made it possible to propose, manufacture and test tools with aperiodic arrangement of single diamond grains.

The studies were performed until the complete destruction of the surface diamond-containing layer, which allowed obtaining a certain statistical sample to determine the parameters of the model of failure at

$$P(T) = \left[ 0,5 + \Phi \left( \frac{X_{max} - a_0 - \gamma_{cp}T}{\sqrt{\sigma_a^2 + \sigma_\gamma^2 T^2}} \right) \right] \cdot e^{-\lambda T} \quad (9)$$

Since actually one sample of the tool was tested, the reliability of the results is 95%.

The comparison of the characteristics of the tools is illustrated by the following dependences (Fig. 11).

If the productivity of the process, determined at a fixed working feed or a fixed cutting force (in this case 15 N) is taken as parameter  $X_{max}$ , a decrease in productivity less than by 1  $\text{mm}^3/\text{s}$  can be considered a parametric failure.

Then  $a_0 = 0,27$ ,  $\sigma_a = 0,045$ ,  $\gamma = 0,00037 \text{mm}^3/\text{s}$ ,  $\sigma_\gamma = 0,000012$  and the expected flow of failures  $\lambda = 0,000025$ .

It becomes obvious that the proposed engineering solutions work more stably and are less susceptible to contamination on work surfaces. This is also evidenced by microphotos of the working surfaces of the tool. However, the dependences are quite different, which necessitates a multifactorial experiment that would link the factors taken

into account ( $t, h, w, v, p$ , see Table 4) with the processing efficiency parameter  $Q$ ,  $mm^3/s$ .

The factors taken into account on the boundary of their variation are given in Table 5, and the results of statistical processing – in Fig. 12.

Statistical processing of the results of the experimental plan allowed building the following regression dependence:

$$Q = 1,193 + 1,625h + 0,00857143p + 0,015625v - 0,0017W \quad (10)$$

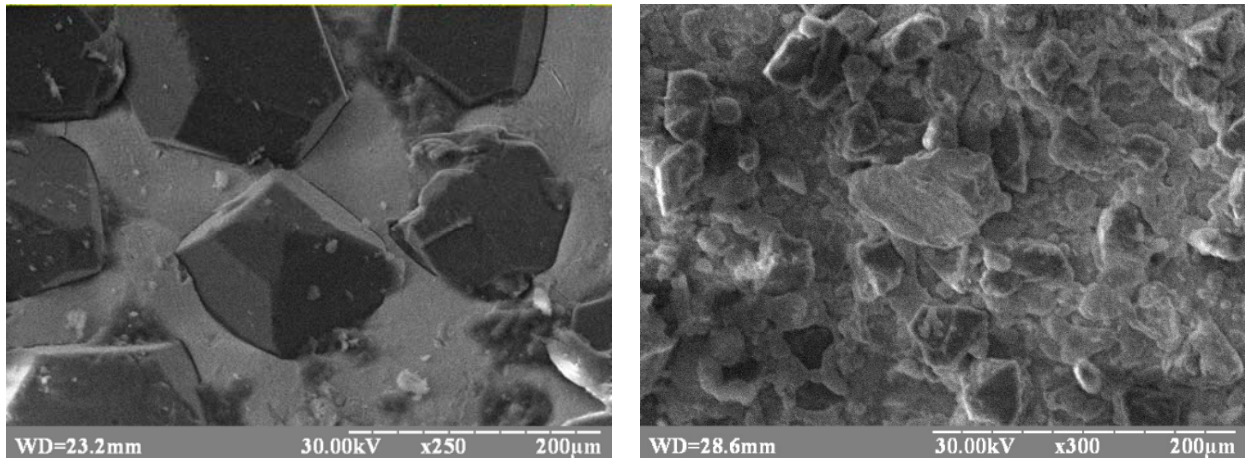


Fig. 10. Formation of clusters with the laying of grains on a flat surface

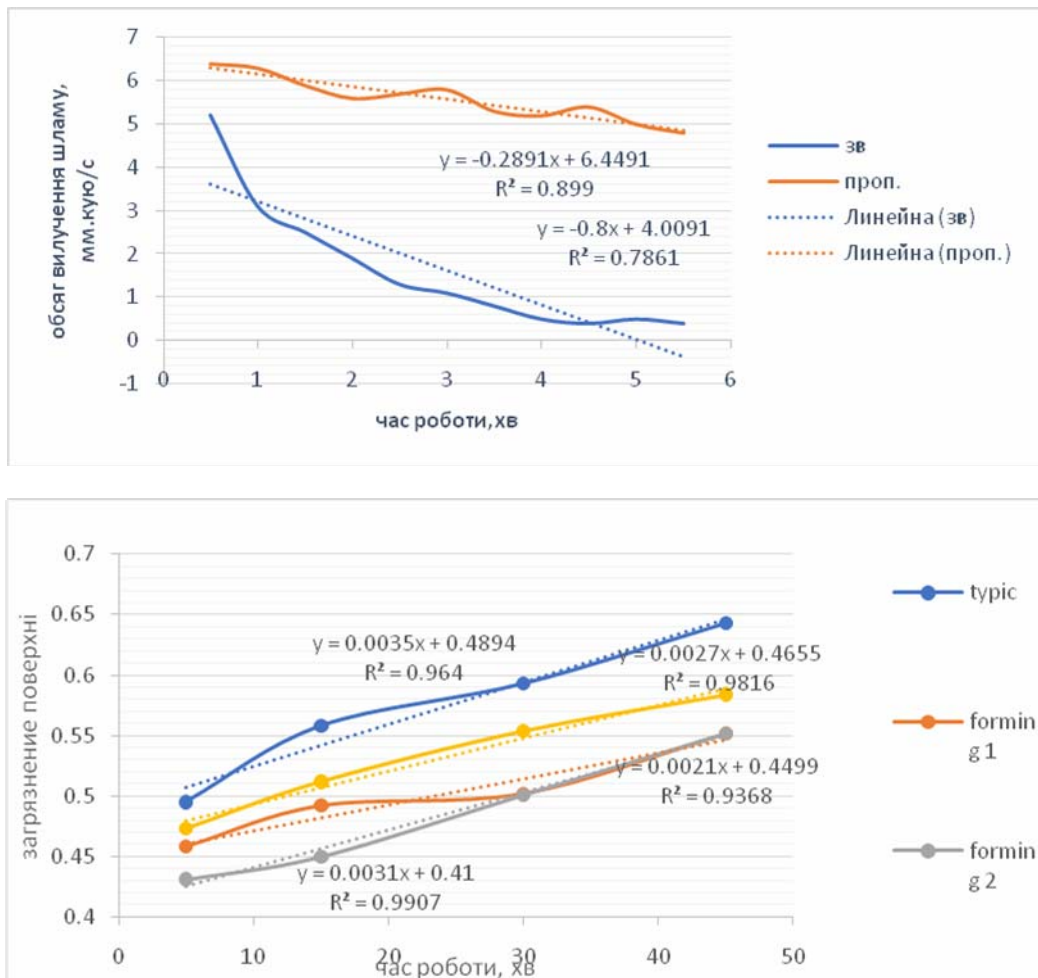
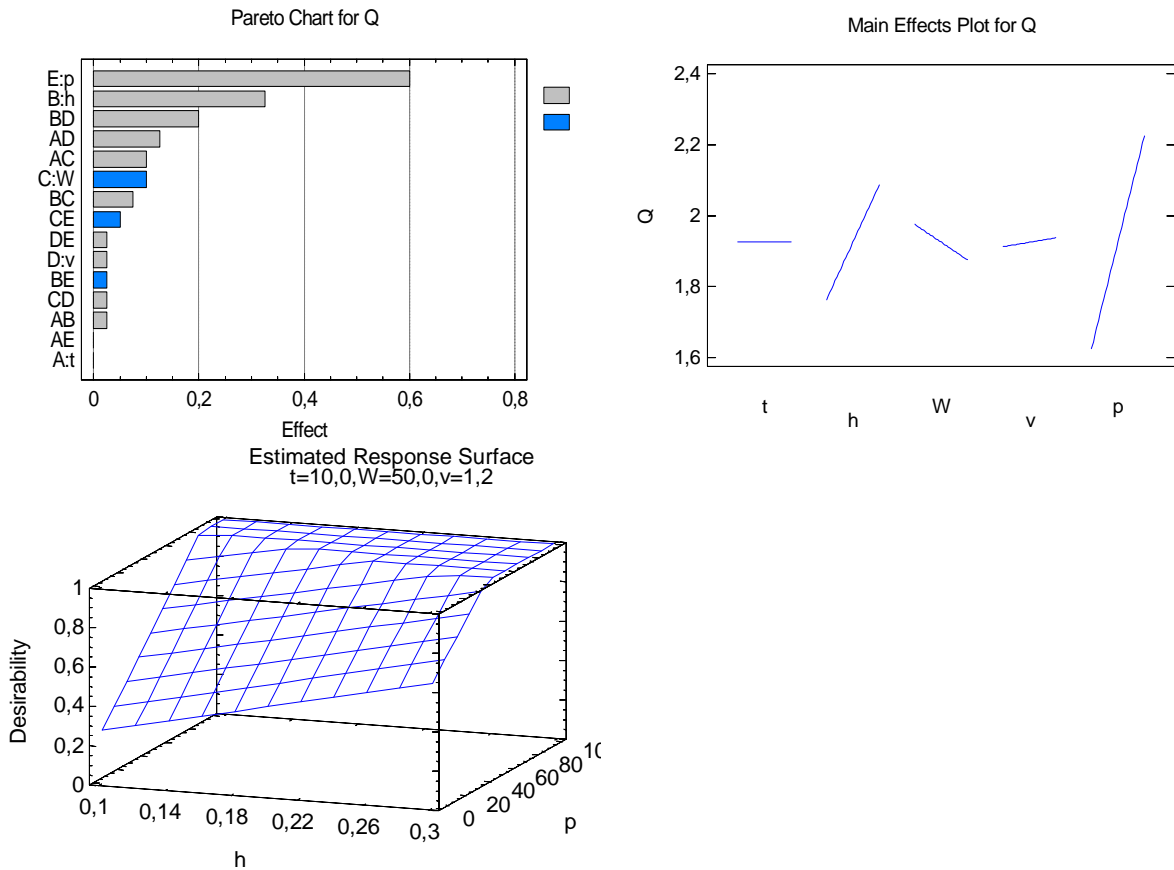


Fig. 11. Change in cutting productivity (a) and increase in contamination of the tool surface (b) for the proposed tool and the conventional one

**Table 5** Boundaries of variation of the factors taken into account

Factor		Designation	Measurement	max	min
1	Cluster step	$t$	mm	3	15
2	Grains escape	$h$	mm	0.05	0.1
3	Density of laying on a surface	$w$	%	20	80
4	Speed of movement	$v$	m/s	0.4	2.0
5	Tool pressing force	$P$	N	20	90
Parameter відгук		$Q$	$\text{mm}^3/\text{s}$		



*Fig. 12. The degree of influence of factors (a), their main effects are the response surface*

Compared with the conventional tool, it can be stated that the proposed one has a lower rate of damage, and the initial scattering of parameters is also 27-32% less.

It becomes obvious that the proposed engineering solutions work more stably and are less susceptible to contamination on work surfaces. This is also evidenced by microphotos of the working surfaces of the tool. However, the dependences are quite different, which necessitates a multifactorial experiment that would link the influencing factors with the parameter of processing efficiency. In view of the above, it is reasonable to reengineer the creation of the cutting surface. At the same time sites and zones of the maximum thermobaric loading are defined, and the cluster of a surface is constructed according to working conditions.

It is shown that the errors of the simulation and the obtained regression models do not exceed 5-7%, and the use of a tool based on a functional approach is 20-25% higher for ring drills, 40-50% for flexible tools (diamond strings) and 15-20% for elastic tools (renovator saws).

**CONCLUSIONS**

The results of research of the process of laser thermodeformation sintering for the formation of reliable surface clusters of the minimum required size are given (which proved the third scientific position). Its properties change according to the forecast dependences. The model and experimental results have been compared as to the surface properties. It has been shown that the errors of the simulation and the obtained regression models do not exceed 5-7%, and the use of the tool created on the basis of the functional approach is higher by 20-25% for ring drills, by 40-50% for flexible tools (diamond strings) and by 15-20% for elastic tool (renovator saws).

**REFERENCES**

[1] Heifets M.L., Kolmakov A.G., Vityaz P.A., Senyut V.T., Klimenko S.A. Improving the technology of obtaining diamond nanostructured materials using physico-chemical nonequilibrium analysis *Materialovedenie, Nauka i tehnologii* (2015) 42-47

- [2] Verezub N.V., Tarasiuk A.P., Khavyn H.L., Hetmanov A.A. Mechanical processing of fiber polymer composites: Monograph Kharkiv KNADU (2001) 180
- [3] Lord E.E., Mackey A.L., Ranganatan S. New geometry for new materials / trans.from Eng. Ed. by V.Ya. Shevchenko, V.E. Dmytryienko M. Fizmatlit (2010) 360 ISBN 978-5-9221-1243-7
- [4] Salenko A., Shchetynin V., Gabuzian G., Lashko E., Mohamed RF Budar, Klimenko S., Potapov A. Cutting Superhard Materials by Jet Methods (on Functional Approach). Recent Advancements in the Metallurgical Engineering and Electrodeposition. IntechOpen (2019) 1-21
- [5] Norbert G., Paulo D., Tibor S. Advanced cutting tools and technologies for drilling carbon fiber reinforced polymer (CFRP) composites: A review. Composites Part A: Applied Science and Manufacturing. 125 (2019) 105552 <https://doi.org/10.1016/j.compositesa.2019.105552>
- [6] Dhand V., Mittal G., Rhee K.Y., Park S.J., Hui D. A short review on basalt fiber reinforced polymer composites. - Composites Part B: Engineering 73 (2015) 166-180
- [7] Skeebe V.Yu., Ivancivsky V.V., Lobanov D.V., Zhigulev A.K., Skeebe P.Yu. Integrated processing: quality assurance procedure of the surface layer of machine parts during the manufacturing step "Diamond smoothing" - IOP Conf. Series: Materials Science and Engineering 125 (2016) 012-031
- [8] Yuanyushkin A.S., Rychkov D.A., Lobanov D.V. Surface quality of the fiberglass composite material after milling. - Applied mechanics and materials 682 (2014) 183-187
- [9] Arkhipov P.V., Yanyushkin A.S., Lobanov D.V., Petrushin S.I. The effect of diamond tool performance capability on the quality of processed surface. Applied mechanics and materials 379 (2013) 124-130
- [10] Hrabchenko A.I., Dobroskok V.L., Fedorovych V.A. 3D simulation of diamond abrasive tools and grinding processes: Textbook. — Kharkiv: NTU “KPI” (2006) 364
- [11] Integrated generative technologies: textbook [for HEI students] / Hrabchenko A.I., Vnukov Yu.N., Dobroskok V.L. [et al.]; ed. by A.I. Hrabchenko. — Kharkiv: Hrabchenko A.I., Dobroskok V.L., Fedorovych V.A. 3D simulation of diamond abrasive tools and grinding processes: Textbook. — Kharkiv: NTU “KPI” (2011) 416
- [12] Textbook. —Kh.: NTU “KPI” (2009) 230
- [13] Dobroskok V.L., Shpylka A.N., Poltava, Ukraine, V.B. Kotliarov, Obtaining a triangulation model of the relief of the working surface of grinding wheels. - Cutting and tooling in technological systems 84 (2014) 85-92
- [14] Orel V.N., Shchetynin V.T., Salenko A.F., Yatsyna N.N. The use of controlled cracking to improve the efficiency of waterjet cutting. Eastern-European Journal of Enterprise Technologies 1 (7) 45-56
- [15] Altshuller H.S. Find the idea: Introduction to the theory of solving an inventive problem. Novosibirsk: Nauka (1991) 225
- [16] Mykhailov A.N., Mykhailova E.A., Madzhyd A.D. Features of the synthesis of the structure of functionally oriented technological processes of combined finishing processing of axial blade tools. High technologies in mechanical engineering: Collected papers NTU “KPI”. – Kharkiv: NTU “KPI” 1 (18) (2009) 131–150.
- [17] Mykhalov A.N., Al-Sudani T.T., Mykhailov D.A., Dolhikh A.S. Methods for increasing the tool life and / or productivity of cutters with variable cutting speeds along the length of the cutting edge of the tooth // Advanced technologies and systems in mechanical engineering: International collection of papers. – Donetsk: DonNTU, 1 (2) (45) (2013) 173–180
- [18] Shchetynin V.T. Kyrychenko A.M., Metak Al Ibrakhim., Chencheva O.O. Regularities of formation of initial indicators of quality at processing of leaky carbon-containing materials by the abrasive tool – Bulletin of Kremenchuk Mykhailo Ostrohradskyi National University. - Kremenchuk: KrNU 1 (114) (2019) 41-49
- [19] Salenko A., Chencheva O., Gluchova V., Schetynin V., Mohamed RF Budar, Klimenko S., Lashko E.. Effect of slime and dust emission on micro-cutting when processing carbon-carbon composites. Eastern-European Journal of Enterprise Technologies 3/1 (105) (2020) 38–51.
- [20] Sheikh-Ahmad J., Paulo Davim J. Cutting And Machining of polymer Composites, Wiley Encyclopedia of Composites, 2012.
- [21] Meijer J., Van Sprang I. Optimization of Laser Beam Transformation Hardening by One Single Parameter. - CIRP Annals. 40 (1) 1991 183-186. [https://doi.org/10.1016/S0007-8506\(07\)61963-5](https://doi.org/10.1016/S0007-8506(07)61963-5)
- [22] Kaplya V.I., Pan A.G., Dyagileva T.G. Algorithm for calculating the minimum time of one stroke of a stepper motor. Injenernii vestnik Dona 2 (2015) – [ivdon.ru/ru/magazine/archive/n2y2015/2943](http://ivdon.ru/ru/magazine/archive/n2y2015/2943)